Journal of Sound and Vibration (1998) **210**(2), 267–278

DETECTION OF STRUCTURAL FAULTS BY MODAL DATA, LOWER BOUNDS AND SHADOW SITES

T. Contursi and L. M. Mangialardi

Dipartimento di Progettazione e Produzione Industriale, *Politecnico di Bari*, 70126 *Bari*, *Italy*

and

A. Messina

Dipartimento di Scienza dei Materiali, *Università di Lecce*, 73100 *Lecce*, *Italy*

(*Received* 24 *January* 1997, *and in final form* 18 *September* 1997)

Different algorithms have recently been developed for the diagnosis of many types of civil and mechanical structures using modal data, such as natural frequencies and mode shapes. Although many solutions have been proposed, some important questions seem to be absent in the technical literature. If changes in a structure's modal parameters are able to reflect structural faults, it is important to know what is the smallest detectable physical change in that structure.

It is suggested that damage detection by means of modal data can be useful for macro-damage rather than for micro-damage. This resulted from numerical and experimental tests using a simple correlation between measurement noise and sensitivity of modal data, with respect to structural changes in different parts of a sytem. An automatic sensitivity approach is presented to obtain the lower bound of structural faults for the particular structure under study. The same automatic procedure is able to detect possible shadow sites within the frequency range analyzed.

1. INTRODUCTION

When local damage occurs on single or multiple sites of a structure, its static and dynamic behaviour may change significantly depending on the size of the damage and its location. Consequently, static and/or dynamic parameters should be monitored to readily detect the problem so that adequate preventive measures may be taken. It is important to detect damage at its early stages so as to have a longer lead time to final failure.

Recently dynamic parameters, such as modal data, have been extensively used (for a short review see references [1–9]) with different approaches, different amounts of data, and differing advantages and disadvantages. Of particular importance is reference [3] where about 300 references covering the past 20 years are critically discussed. Although all these methods acknowledge the importance of validating measurement errors by using real data from measurements on real structures, no information has been reported about the smallest physical change in a structure which may be detected from changes in its modal parameters. It would also be interesting to explore whether damage in any location on a structure may be detected by modal parameter changes when a reduced frequency range is available, as is practically always the case.

Some authors acknowledge the importance of the problem. Richardson and Mannan [10] point out that the best answer is, "*The smaller the better!*", assuming that it is always

0022–460X/98/070267 + 12 $25.00/0/sv971303

better to detect damage at its early stages. Experimental tests [10] have been carried out to show that modal data can be effective in detecting the slightest structural changes. No automatic method was however introduced to measure the smallest detectable change.

Also Farrar and Cone [11] felt the need to quantify the amount of damage that causes measurable changes in modal parameters. This work was carried out principally from an experimental point of view (for a bridge) in order to provide the scientific community with real data as a tool for benchmarking damage detection algorithms.

By using a projectile launched from a low pressure compressed air tube, Tracy *et al*. [12] investigated the effects of impact damage on composite materials. Although small local defects showed significant and different changes in the natural frequencies which fell within the range analyzed, they recognized that further work was necessary to determine whether the modal inspection technique could resolve fine variations in the size and location of impact damage.

By relating measurement noise to the sensitivity of damaged sites, this paper proposes an automatic procedure to assess the lowest amount of damage detectable on a structure. The numerical and experimental tests illustrated suggest using the same automatic procedure to check whether there are any shadow sites, i.e., sites where potential damage cannot be detected by the modal data of a given frequency range.

Since it is difficult to group the various types of damage into one single representative class, all the assessments were made using a stiffness reduction factor to implement a homogeneous reduction of stiffness. Finally, the case for which any location of the structure has the same probability to be damaged is investigated, as well as the case for which loads and stresses are not easily predictable.

2. CHARACTERIZATION OF THE SENSITIVITY OF THE STRUCTURE

When the health state of a key machine for a production cycle or an important structure has to be monitored, a simple procedure may be used to determine whether damage is present on the structure. Until damage is detected the location and size of the damaged sites would be uncertain and meangingless.

A simple way to detect whether a fault has occurred on a structure (using modal analysis techniques) is to look for possible shifts in the natural frequencies considered. This subset of modal parameters, i.e., natural frequencies, has been chosen because they cost less than measuring mode shapes and the noise threshold is lower than the one which characterizes damping measurements and mode shapes [11].

The noise threshold in a set of natural frequencies may be estimated by measuring a set of FRFs with different pairs of measuring points on the structure under study.

A necessary condition to detect the jth damaged site by checking the kth natural frequency change is:

$$|\delta f_k(\delta D_j)| > \sigma_k. \tag{1}$$

If the standard deviation σ_k, of the kth natural frequency in a set of FRFs functions is assumed to be proportional to the frequency value, equation (1) can be rewritten as:

$$\frac{|\delta f_k(\delta D_j)|}{f_k} > \frac{\sigma_k}{f_k} = \varepsilon, \tag{2}$$

with a constant or maximum percent band error threshold ε for any kth frequency. In order to assess whether the mesh of an FE model in all the j sites involves a significant change in modal data and thus verify equation (2), it is necessary to evaluate the first member of the equation.

Hence, a damage site is introduced by using homogeneous stiffness reduction factors D_j for the jth stiffness matrix. When small faults occur with a particular scenario on the structure, the kth natural frequency changes as follows:

$$\delta f_k(D_1, D_2, \ldots, D_m) = \frac{\partial f_k}{\partial D_1} \cdot \delta D_1 + \frac{\partial f_k}{\partial D_2} \cdot \delta D_2 + \cdots + \frac{\partial f_k}{\partial D_m} \cdot \delta D_m. \tag{3}$$

When the stiffness change occurs at a single site only, the kth frequency change δf_k is directly proportional to the sensitivity $\zeta_{kj} = \partial f_k / \partial D_j$ term. A single damage site transforms condition (2) into (4):

$$\frac{|\delta f_k|}{f_k} = \frac{1}{f_k} \cdot \frac{\partial f_k}{\partial D_j} \cdot |\delta D_j| = \frac{1}{f_k} \cdot \zeta_{kj} \cdot |\delta D_j| > \varepsilon. \tag{4}$$

Thereby the minimum detectable damage in location j is:

$$(\delta D\%_{k,j})_{min} = \frac{f_k \cdot \varepsilon\%}{\zeta_{kj}}. \tag{5}$$

With equation (5) the minimum detectable damage may be readily estimated by using natural frequencies and sensitivity terms, ζ_{kj}. The latter can be assessed by running one eigensolution of the FE model supposing the structure is in an undamaged state. This possibility is reported in the following section.

Further perusal of equation (5) makes it clear that the existence of a lower bound of damage with respect to the noise threshold is related to the behaviour of the sensitivity term ζ_{kj}. This term, as will be clarified further on, is different from zero when no local rigid body motion is present and it decreases monotonically to zero when the size of the elements used to characterize the damaged sites is small.

By using equation (5) a matrix $\mathbf{C}$ can be defined. For each jth column it reports the minimum detectable damage at location j by checking the kth frequency change. By adding a complementary row in $\mathbf{C}$ $[p + 1 \times m]$, that is the minimum for each column j, it is possible to get an indication of shadow sites, or the location j for which $\mathbf{C}_{p+1,j} > 100\%$ (it is impossible that damage exceeds a complete loss of the element itself). Occasional damage at that location j will never be detected by checking the natural frequency changes.

This last observation is obviously constrained by a first order approximation. The minimum detectable stiffness change, assessed by (5), has been obtained by equation (3), where the frequency change, δf_k, is determined by making use of a first order approximation. Thus, if the calculation is made to obtain lower bounds of damage and consequently a very small δD_j change, estimation of the elements in $\mathbf{C}$ will be fairly good. The same does not apply when high values of δD_j are assessed, as when shadow sites are estimated. Nevertheless, good estimations can also be obtained for shadow sites, as is shown later in this paper.

2.1. SENSITIVITY PROPERTIES AND EXISTENCE OF LOWER BOUNDS FOR DETECTABLE FAULTS

Modelling a damaged site by introducing homogeneous stiffness reduction factors D_j, but no damage in the mass matrix, a global matrix in structural co-ordinates can be assembled with a classical FE assembly procedure as follows:

$$[\mathbf{K}] = \sum_{j=1}^{m} [\mathbf{A}]_j^T D_j [\mathbf{K}]_j [\mathbf{A}]_j = \sum_{j=1}^{m} D_j [\mathbf{K}]_j^P, \tag{6}$$

where the Boolean assembly matrices $[\mathbf{A}]_j$ position the terms from each element matrix within the global matrix.

It can be shown [13] that the sensitivity of the kth eigenvalue to a small stiffness change in the jth element is

$$\xi_{kj} = \frac{\partial \lambda_k}{\partial D_j} = \frac{\{\phi_k\}^T [\mathbf{K}_j]^P \{\phi_k\}}{\{\phi_k\}^T [\mathbf{M}] \{\phi_k\}}, \tag{7}$$

or, equivalently, with respect to the natural frequencies:

$$\zeta_{kj} = \frac{\partial f_k}{\partial D_j} = \frac{1}{8 \cdot \pi^2 \cdot f_k} \frac{\{\phi_k\}^T [\mathbf{K}_j]^P \{\phi_k\}}{\{\phi_k\}^T [\mathbf{M}] \{\phi_k\}}. \tag{8}$$

By means of (7 and 8) a sensitivity matrix—**[S]** or **[s]** respectively —can be assessed by obtaining just one eigensolution of the system.

As shown in reference [5] and mentioned here for completeness from another point of view, by using equations (7 and 8), the following additive property can be proved:

The sum of all the elements in the kth row of **[S]** *is equal to the eigenvalue* λ_k *and the sum in the kth row of* **[s]** *is equal to* $f_k/2$.

1. **Proof**

By considering the classical eigenvalue problem for an undamaged structure:

$$([\mathbf{K}] - \lambda_k [\mathbf{M}])\{\phi_k\} = \{0\}. \tag{9}$$

Re-arranging and pre-multiplying by $\{\phi_k\}^T$ we obtain,

$$\{\phi_k\}^T [\mathbf{K}] \{\phi_k\} = \lambda_k \{\phi_k\}^T [\mathbf{M}] \{\phi_k\}. \tag{10}$$

Using equation (6) in (10) and comparing the result with equation (7), we have:

$$\lambda_k = \frac{\{\phi_k\}^T \sum_{j=1}^{m} [\mathbf{K}_j]^P \{\phi_k\}}{\{\phi_k\}^T [\mathbf{M}] \{\phi_k\}} = \frac{\sum_{j=1}^{m} (\{\phi_k\}^T [\mathbf{K}_j]^P \{\phi_k\})}{\{\phi_k\}^T [\mathbf{M}] \{\phi_k\}} = \sum_{j=1}^{m} \xi_{kj}. \tag{11}$$

Moreover, if equation (8) is recalled, we can write:

$$\lambda_k = \sum_{j=1}^{m} \xi_{kj} = \sum_{j=1}^{m} \zeta_{kj} \cdot 8 \cdot f_k \cdot \pi^2, \tag{12}$$

and considering the independence of the k index with respect to the j index we obtain:

$$\lambda_k = (2 \cdot \pi \cdot f_k)^2 = 8 \cdot f_k \cdot \pi^2 \cdot \sum_{j=1}^{m} \zeta_{kj}, \tag{13}$$

and finally,

$$\sum_{j=1}^{m} \zeta_{kj} = \tfrac{1}{2} \cdot f_k. \tag{14}$$

□

This property of the eigenvalues outlined in equations (12) and (14) suggests an interesting observation:

The sensitivity of any natural frequency to changes in any element of a structure corresponds to a fraction of the eigenvalue amongst all the finite elements with which the structure has been modelled.

Given that natural frequencies are unchangeable physical properties of a structure, a refinement of the mesh into smaller sites reduces any positive semi-definite term of the [**s**] matrix, supposing that the higher convergence of the redefined mesh is neglected. Hence, using equation (5), it is evident that a lower bound, $\delta D_{kj,min}$, exists for the minimum extent of damage beyond which it is impossible to detect significant changes in natural frequencies when damage occurs on the structure.

Finally, from a computational point of view, equation (5) proves to be efficient in estimating the size of damaged and potential shadow sites. Indeed, owing to the additive property mentioned above, estimation with a rough mesh is always better than with a finer one because the following inequalities are always verified:

$$\zeta_{k,j}^{\text{rough mesh}} \geqslant \zeta_{k,j}^{\text{finer mesh}} \overset{(5)}{\Rightarrow} (\delta D_{k,j}^{\text{rough mesh}})_{min} \leqslant (\delta D_{k,j}^{\text{finer mesh}})_{min}. \tag{15}$$

Consequently, if damage at location j is not detectable, then the damage extent cannot be detected in a site within the same jth location. Hence, a rough analysis which relies on the finite elements used is able to isolate areas where shadow sites are certainly located.

3. NUMERICAL AND EXPERIMENTAL EXAMPLES

If a fact has been proven theoretically, its usefulness must be validated experimentally. Two numerical examples have been considered in this investigation. Corresponding experimental validations prove the usefulness of the method proposed to estimate the smallest detectable damage in a mechanical system.

The first example concerns a cantilever beam. This structure has been chosen because of its manifold applications. In this case, experimental confirmation comes from the existing literature [14].

The second example is a completely free aluminium angled beam for which only out-of-plane vibrations have been considered. In this case full numerical and experimental assessments and corresponding comparisons have been carried out.

All the assessments were performed by introducing $E = 70$ GPa, $v = 0{\cdot}3$, $\rho = 2770$ kg/m^3 into the numerical models.

3.1. CANTILEVER BEAM MODEL

Figure 1 shows the numerical model used and the corresponding FE-mesh with three different discretizations, using 10, 20 and 30 elements. The same picture also illustrates the material and the geometric properties applied. The corresponding natural frequencies are listed in Table 1. Owing to the high h/L ratio, the assessments have been carried out by using the Eulero–Bernoulli model by an FE package developed in house, hereafter indicated as FE/built-in package.

Figure 2 shows the additive property presented in section 2.1 relative to the first frequency. The **C** matrix was assessed by using a subroutine implemented in an FE/built-in package, the same used to assess the natural frequencies listed above. The results are listed in Table 2. A band error of 1·0% was used to estimate the lower bounds of the damage that significantly influenced the first ten natural frequencies in the frequency range of about

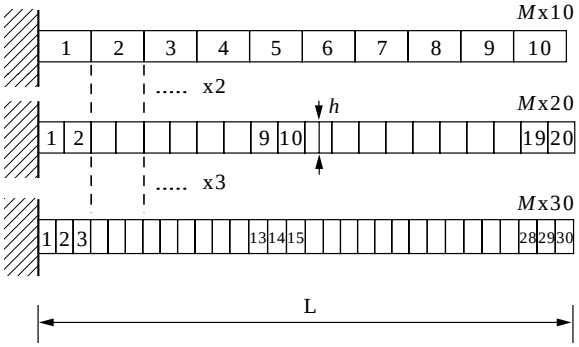

Figure 1. Cantilever beam FE-model with material and geometric properties. Analytical base for FE model: bending vibration: Eulero model; longitudinal vibration: no transverse effect. $E = 70$ GPa, $\rho = 2770$ kg/m^3, $h/l = 1/50$, $L = 500$ mm, cross-section = rectangular.

6·5 kHz. In order to clearly show the critical sites (Table 2), minimum damage values higher than 60% are in bold type.

As shown in Table 2, it is difficult to introduce significant changes in the first mode when local damage occurs in locations 6–10. A stiffness reduction in locations 7–10 will never change the first natural frequency significantly. A similar behaviour shall be expected if the first three mode shapes are taken into account to check the integrity of the extremity of the cantilever beam.

If the first six mode shapes are taken into account the **C** matrix indicates that damage at location 10 will never be detected due to the shifts of the corresponding natural frequencies. Location 10 is a shadow site in the 2·5 kHz range, but not in the 6·5 kHz range.

Similar results were suggested by Rizos *et al*. [14] whose work introduced a method to locate a crack on a beam and was followed by a numerical–experimental test. Rizos *et al*. reported that the biggest localization errors, after damage had occurred, were at the extremity of a cantilever beam specimen. Our work has shown that modal data in a cantilever beam have a low sensitivity to the first natural frequencies.

3.2. ANGLED BEAM MODEL

Figure 3 depicts the numerical model used to simulate the dynamic behaviour of an aluminium angled beam specimen during free out-of-plane vibrations. The same picture shows the FE model with beam elements connected by 13 nodes and 12 elements.

TABLE 1

Natural frequencies (Hz) of the cantilever model (Figure 1)

No	Type	Analytical	FE-M × 10	FE-M × 20	FE-M × 30
1	Bent	32·5	32·5	32·5	32·5
2	Bent	203·6	203·8	203·8	203·8
3	Bent	570·0	570·7	570·6	570·6
4	Bent	1116·9	1119·1	1118·1	1118·1
5	Bent	1846·4	1852·9	1848·5	1848·3
6	**Long**	**2513·5**	**2516·1**	**2514·1**	**2513·8**
7	Bent	2758·2	2775·8	2762·0	2761·2
8	Bent	3852·3	3894·6	3859·0	3856·8
9	Bent	5128·9	5217·8	5140·5	5135·3
10	Bent	6587·7	6746·5	6607·9	6597·1

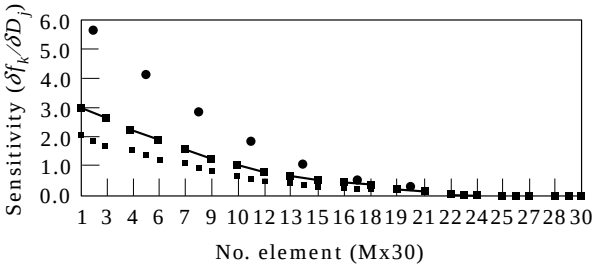

Figure 2. Sensitivity of the first frequency (32·5 Hz) with respect to any finite element for each mesh considered in Figure 1. ●, M × 10; M × 20; –■–, M × 30.

TABLE 2

C matrix containing the minimum detectable fault by measuring natural frequency changes when a threshold error ε% of 1% *is considered* (*reference*: *Figure* 1, *M* × 10)

	*j*th location									
*k*th	1	2	3	4	5	6	7	8	9	10
1	5·76	7·91	11·51	18·02	31·09	**61·43**	**148·27**	**495·38**	**3068·98**	**89784·07**
2	8·35	48·40	**168·10**	22·52	11·28	9·89	13·22	28·19	**123·94**	**2796·21**
3	11·83	**114·08**	15·49	13·75	**63·08**	48·41	10·95	9·88	26·27	**435·18**
4	16·34	25·20	14·25	**105·44**	14·52	14·73	**94·64**	11·42	12·91	**141·61**
5	20·27	15·12	43·11	15·02	22·33	22·58	15·37	36·23	10·21	**66·02**
6	10·06	10·58	11·72	13·76	17·29	23·71	36·63	**68·28**	**183·50**	**1624·48**
7	21·61	15·47	33·07	15·83	22·01	21·91	16·03	33·59	11·56	38·46
8	20·51	21·36	15·31	34·25	16·81	16·88	34·27	15·59	16·76	26·18
9	18·73	26·84	16·89	17·07	24·73	24·55	16·97	17·24	22·87	20·11
10	17·66	22·58	21·42	20·29	19·38	19·41	20·37	21·64	21·26	17·34
10 + 1	5·76	7·91	11·51	13·75	11·28	9·89	10·95	9·88	10·21	17·34

Note: **C** matrix: $(\delta D\%k, j)_{min}$, $\varepsilon\% = 1{\cdot}0$.

All the assessments were carried out using the same FE/built-in package mentioned in section 3.1. In order to have a complete data-base for comparison, the assessments were also carried out using a commercial FE/package: Ansys V.5.0 which modelled the specimen under investigation by using 3-D solid elements (SOLID45).

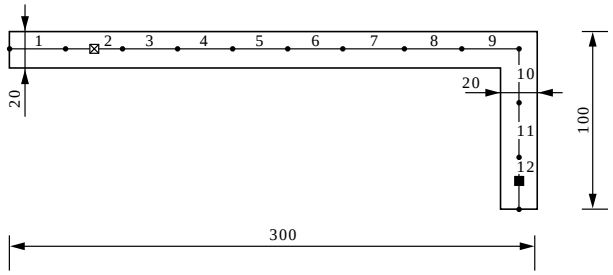

Figure 3. Angle beam FE-model with geometric characteristics (all dimensions in mm). ■, Response point; ⊠, Impact point. Thickness 10 mm.

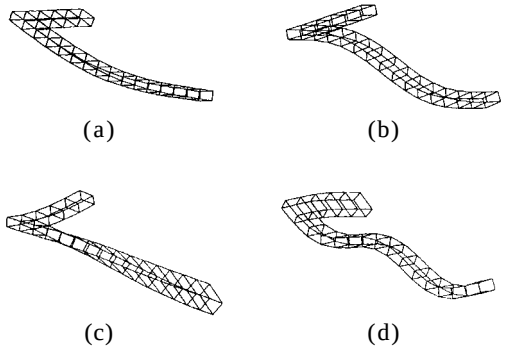

Figure 4. Mode shapes, out-of-plane vibrations of the angle beam model. (a) Mode 1: 537·0 Hz. (b) Mode 2: 1514 Hz. (c) Mode 3: 2113 Hz. (d) Mode 4: 3024 Hz.

The values obtained with Ansys V.5.0 are shown in Figure 4, where the first four mode shapes and the natural frequencies are reported together. The natural frequencies resulting from the FE/built-in package are listed in Table 3 together with the Ansys values and the experimental natural frequencies.

3.2.1. *Angle beam model, experimental and numerical comparisons*

Three specimens with the same geometric characteristics depicted in Figure 3, were obtained from the same square aluminium plate. For each one of them a different element was damaged and for each damage stage the natural frequency changes were assessed by the impulse hammer technique [15]. Figure 3 also shows the measuring point pair (the response point—for the location of the accelerometer, and the impact point—for the location where the hammer was impacted) used to measure the frequency response functions (H2–12). The latter were estimated by averaging five subsequent measurements at each stage of the damaged or undamaged state.

In Figure 3, the specimens called (a), (b) and (c) were respectively damaged in element nos 5, 9 and 12. A homogeneous reduction in stiffness was simulated by removing, on an out-of-plane side of the specimen. Uniformly 0·5 mm of material was removed three times corresponding to about 15%(−0·5 mm), 30%(−1·0 mm) and 40%(−1·5 mm) of damage.

A circle fitting procedure based on the concept of a single degree of freedom [15] (SDOF) was carried out in the complex plane to extract the first four experimental natural frequencies. Because of the separation among the natural frequencies detected in the frequency range analyzed, the SDOF procedure described should ensure confident results. Table 3 shows all the experimental and numerical results to show the natural frequency values of the undamaged state, and Table 4 reports the percentage of natural frequency

TABLE 3

Comparison between experimental and numerical natural frequencies (*Hz*) (*reference*: *Figure* 3, *undamaged state*)

Mode no.	Specimen (a)	Specimen (b)	Specimen (c)	FE-Ansys 3-D	FE-beam Bernoulli
1	570·6	567·4	550·0	537·0	541·7
2	1573·0	1565·0	1515·0	1514·0	1503·0
3	1989·0	1992·0	1975·0	2113·0	1938·0
4	3040·0	3024·0	2929·0	3024·0	2934·0

TABLE 4

Percentage frequency changes when a damage occurs in a single site only on the alluminium angle beam shown in Figure 3

	Damage element no. 5 specimen (a)			Damage element no. 9 specimen (b)			Damage element no. 12 specimen (c)		
Mode no.	15%	30%	40%	15%	30%	40%	15%	30%	40%
1	−1·49	−3·66	−6·29	+0·30	+0·32	+0·42	+0·16	+0·16	+0·15
2	−0·19	−0·40	−0·70	−0·30	−0·75	−1·34	+0·15	+0·14	+0·25
3	−0·48	−0·90	−1·53	−1·30	−2·51	−4·32	+0·20	+0·28	+0·48
4	−0·83	−2·66	−2·91	−0·77	−1·68	−3·02	+0·19	+0·29	+0·45

changes assessed experimentally in the undamaged state. In Figure 5 the log–lin inertance plot of the three cases (a–c) considered in this work shows clearly the percentage frequency shifts listed in Table 4 with a 40% damage level. Finally, Table 5 shows the **C** matrix that represents a prediction of the sensitivity of the modal data used to check the health state of a structure by utilizing the first four natural frequencies of the system.

From the diagnosis of the plots shown in Figure 5, it's clear that in the 0–4 kHz range, the presence of 40% damage on element no. 12 could not be detected. The natural

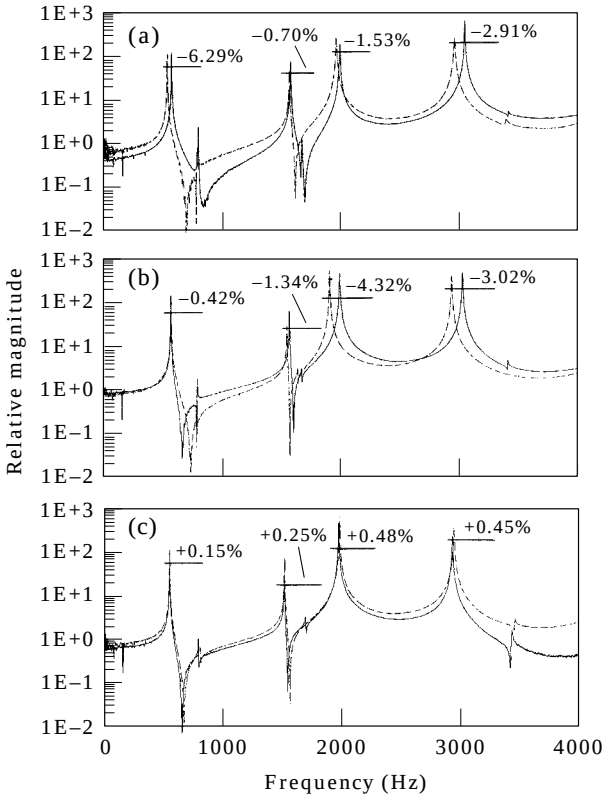

Figure 5. Plot of experimental FRFs of the intact and damaged angle beam with about 40% stiffness reduction in different locations. ——, FRF (H2–12) undamaged. (a) ---, FRF (H2–12) damaged element no. 5. (b) – – –, FRF (H2–12) damaged element no. 9. (c) ————, FRF (H2–12) damaged element no. 12.

TABLE 5

C *matrix containing the minimum detectable fault by measuring natural frequency changes when a threshold error* $\varepsilon\%$ *of* 0·5% *is considered* (*reference*: *Figure* 3)

	*i*th location											
*k*th	1	2	3	4	5	6	7	8	9	10	11	12
1	**1090·1**	48·6	11·1	5·2	3·9	4·2	6·8	19·3	**157·4**	**4872·8**	**2768·8**	**26036·7**
2	**179·8**	11·4	4·6	6·1	41·4	13·2	4.6	5·9	26·4	**511·4**	**846·8**	**6343·4**
3	**693·5**	**72·8**	28·9	17·7	11·9	8·5	6·9	6·1	5·7	6·7	18·9	**315·2**
4	**62·3**	6·1	6·4	45·9	6·3	10·8	21·0	4·8	10·6	50·4	50·5	**479·5**
4 + 1	**62·3**	6·1	4·6	5·2	3·9	4·2	4·6	4·8	5·7	6·7	18·9	**315·2**

Note: **C** matrix $(\delta D\%k, j)_{min}$, $\varepsilon\% = 0{\cdot}5$.

frequencies move upwards. This clearly indicates that the stiffness reduction effect does not significantly influence the natural frequency in the analyzed range. The situation is different when damage occurs at locations 5 and 9 (Figures 5(a and b), respectively).

Worth noting is that this behaviour had been predicted in Table 5, where column 12 lists damage higher than 100% to obtain a significant change in natural frequencies with a 0·5% noise threshold [1] for the first four natural frequencies. The similarities with the experimental data, shown in Figure 5 and Table 4, are also applicable to locations 5 and 9.

If specimen (a) (damage in element no. 5) is considered, the **C** matrix in Table 5 indicates that the minimum detectable damage is 3·9% for mode 1 and 6·3% for mode 4, while for modes 2 and 3 the amount of damage introducing a significant natural frequency change is certainly higher. On specimen (a) since small-sized damage is considered (15%), the highest values, like the ones reported in the first column of Table 4, relate only to modes 1 and 4 at any damage stage while the changes in modes 2 and 3 are clearly small.

It is relevant that all the correspondences between numerical and experimental results have been obtained without taking into account updated numerical models, which is a relatively time consuming process. Here, lower bounds and shadow sites have been detected by means of a numerical model. This is in line with Williams *et al*. [16], who pointed out that while experimental natural frequencies could differ from the non-updated numerical FE model, natural frequency changes evaluated on the real system might follow a pattern similar to the estimations carried out with the numerical model.

4. DISCUSSION AND CONCLUSIONS

This survey highlights practical problems in damage detection when using modal parameters. The frequency range is not usually a free choice for the analyst. Quite the contrary, the lowest modes are measurable in the frequency domain from 0 up to maximum frequency value, and the maximum is closely related to the measurement procedure and specimen under investigation. Therefore a method that is able to test the sensitivity of the data base in the available frequency range is obviously welcome.

A numerical and experimental investigation was carried out on the smallest detectable fault by measuring natural frequency changes. The results obtained indicate that modal data may help to detect macro-damage of practical interest. Nevertheless it is the authors' opinion that the frequency range available should be checked before diagnosing the health

state of a structure. This is necessary to understand whether any location of damage is detectable by modal shifts falling in the frequency range analyzed.

An automatic numerical procedure has proven to provide a fairly good estimation of the presence and location of a lower bound of structural faults when a limited frequency range is analyzed. The same automatic procedure is able to detect possible shadow sites within the frequency range considered. The numerical method can be easily implemented in an FE-package requiring only one eigensolution.

ACKNOWLEDGMENTS

The work reported here is part of a national project financed by MURST—40% of the Italian Ministry of University and Scientific and Technological Research. The authors also wish to acknowledge Professor A. Pellerano and Dr S. Pascuzzi of the Institute of Agricultural Machinery of the University of Bari (Italy), who made it possible to carry out all the experimental measurements reported in this work.

REFERENCES

1. A. Messina, I. A. Jones and E. J. Williams 1996 *Proceedings of Identification in Engineering Systems*, *Swansea*, *UK*, 67–76. Damage detection and localisation using natural frequency changes.
2. P. Cawley and R. D. Adams 1979 *Journal of Strain Analysis* **14**, 49–57. The location of defects in structures from measurements of natural frequencies.
3. S. W. Doebling, C. R. Farrar, M. B. Prime and D. W. Shevitz 1996 *Los Alamos National Laboratory Report LA*-13070-*MS*. Damage identification and health monitoring of structural and mechanical systems from changes in their vibration characteristics: a literature review.
4. M. Biswas, A. K. Pandey and M. M. Samman 1989 *The International Journal of Analytical and Experimental Modal Analysis* **5**, 33–42. Diagnostic experimental spectral/modal analysis of a highway bridge.
5. T. Contursi, A. Messina and E. J. Williams 1997 *Journal of Vibration and Control*, in press. A multiple damage location assurance criterion based on natural frequency changes.
6. D. C. Zimmerman and M. Kaouk 1994 *Journal of Vibration and Acoustics* **116**, 222–231. Structural damage detection using a minimum rank update theory.
7. K. G. Topole and N. Stubbs 1995 *The International Journal of Analytical and Experimental Modal Analysis* **10**, 95–103. Non-destructive damage evaluation in complex structures from a minimum of modal parameters.
8. R. G. Cobb and B. S. Liebst 1996 *Proceedings of Identification in Engineering Systems*, *Swansea*, *UK*, 275–284. Structural damage identification using minimal sensor information.
9. N. Stubbs and R. Osegueda 1990 *The International Journal of Analytical and Experimental Modal Analysis* **5**, 67–79. Global non-destructive damage evaluation in solids.
10. M. H. Richardson and M. A. Mannan 1993 *Proceedings of the* 11*th International Modal Analysis Conference* **1**, 893–898. Correlating minute structural faults with changes in modal parameters.
11. C. R. Farrar and K. M. Kone 1995 *Proceedings of the* 13*th International Modal Analysis Conference* **II**, 655–660. Vibration testing of the I-40 bridge before and after the introduction of damage.
12. J. J. Tracy, D. J. Dimas and G. C. Pardoen 1984 *Proceedings of the* 2*nd International Modal Analysis Conference* **I**, 203–209. Advanced composite damage detection using modal analysis techniques.
13. E. J. Williams, I. A. Jones and A. Messina 1996 *Proceedings of Identification in Engineering Systems*, *Swansea*, *UK*, 368–376. Damage detection and localisation using natural frequency sensitivity.
14. P. F. Rizos, N. Aspragathos and A. D. Dimarogonas 1990 *Journal of Sound and Vibration* **138**, 381–388. Identification of crack location and magnitude in a cantilever beam from the vibration modes.

15. D. J. Ewins 1992 *Modal Testing*: *Theory and Practice*, Taunton, Somerset, England: Research Studies Press Ltd.
16. E. J. Williams, A. Messina and B. S. Payne 1997 *Proceedings of the* 15*th International Modal Analysis Conference*, **I**, 652–657. A frequency-change correlation approach to damage detection.

APPENDIX: NOMENCLATURE

[A]	Boolean assembly matrix in FE method
[K]	global stiffness matrix
$[\mathbf{K}_j]^P$	stiffness matrix of jth element positioned in **[K]**
[M]	global mass matrix
m	number of elements in the structure
λ_k	kth eigenvalue (ω_k^2)
$\{\phi_k\}$	kth mode shape
ω_k	kth modal frequency (rad/s)
f_k	kth natural frequency (Hz)
D_j	stiffness reduction factor of jth element
[S]	sensitivity matrix of natural frequencies
[s]	sensitivity matrix of eigenvalues
ξ_{kj}	sensitivity of the kth eigenvalue with respect to the jth stiffness change
ζ_{kj}	sensitivity of the kth frequency with respect to the jth stiffness change

Subscripts

k	mode number, where $k = 1, 2, \ldots, p$
j	element number where $j = 1, 2, \ldots, m$

Superscripts

T	transpose